///VSP/// Journal of Adhesion Science and Technology 26 (2012) 41–54

Journal of ADHESION SCIENCE and TECHNOLOGY
brill.nl/jast

Hydridosilane Modification of Metals: An Exploratory Study

Barry Arkles [a,*], **Youlin Pan** [a], **Yun Mi Kim** [a], **Eric Eisenbraun** [b], **Christopher Miller** [b] **and Alain E. Kaloyeros** [b]

[a] Gelest Inc., 11 East Steel Rd., Morrisville, PA 19067, USA

[b] College of Nanoscale Science and Engineering, The University at Albany–SUNY, 255 Fuller Rd., Albany, NY 12203, USA

Received in final form 23 January 2011

Abstract

The interaction of hydridosilanes with oxide-free metal substrates was evaluated in order to determine their potential for surface modification analogous to alkoxysilanes with metal oxide substrates. Under mild conditions, trihydridosilanes interact with a variety of clean, hydrogenated and fresh metal and metalloid surfaces, including titanium, silicon and gold. In contrast, monohydridosilanes appear to have minimal interaction. All classes of hydridosilanes have minimal interaction with anhydrous oxide surfaces. Preliminary results suggest that surface modification with trihydridosilanes may provide a route for generating self-assembled monolayers on metal substrates. The synthesis of new trihydridosilanes is described. Contact angle, FTIR and XPS data for modified surfaces are provided.
© Koninklijke Brill NV, Leiden, 2012

Keywords

Hydridosilanes, coupling agents, metal surface modification

1. Introduction

The modification of the chemical and physical properties of surfaces with silanes in which the silicon atom has both organic and electronegative substituents, most commonly organofunctional alkoxysilanes, has been an area of intensive investigation [1, 2]. Surfaces that readily undergo transformation by reaction with these silanes are generally considered to be oxide or, more specifically, hydroxyl-rich surfaces that can displace an electronegative substituent on the silicon atom of the silane. The mechanism most frequently invoked for the transformation is one in which a covalent oxane bond is formed between the silane and the substrate, although clearly hydrogen-bond interaction between the silane and substrate hydroxyl groups provides an additional mechanism. Representative applications of silanes are fiber-

* To whom correspondence should be addressed. E-mail: executiveoffice@gelest.com

© Koninklijke Brill NV, Leiden, 2012 DOI:10.1163/016942411X569273

glass treated with organofunctional alkoxysilanes for composites and porous silica treated with alkylchlorosilanes for chromatography.

Nanoscale sequential and hierarchical fabrication methodologies include self-assembled monolayers based on the reaction of the same class of organofunctional alkoxysilanes with oxide surfaces. This class of silanes has little, if any, utility for modification of oxide-free metal substrates. The utilization of alkylthiol for modification of gold substrates introduced by Nuzzo and Allara [3] is widely accepted, but functionality of alkylthiols is limited and the modification of substrates other than gold for nanofabrication has not been reported [4].

The modification of oxide-free metal substrates is an important component in fabrication of nanoscale devices and a more general chemistry for self-assembly would be of obvious utility. A limited number of hydridosilanes with structures analogous to alkylthiols have been reported to modify gold substrates [5]. A mechanism for the modification has not been proposed. While the modification of titanium substrates with hydridosilanes has been reported [6], the titanium surfaces were not oxide-free and the dehydrogenative coupling of the silylhydrides with hydroxyls on the titanium surface according to the following mechanism (1) is responsible for the bonding:

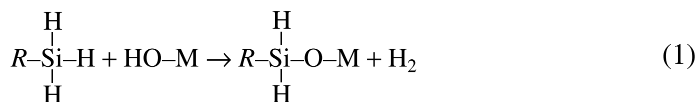

$$R\text{–}\overset{\displaystyle H}{\underset{\displaystyle H}{\mathrm{Si}}}\text{–H} + \text{HO–M} \rightarrow R\text{–}\overset{\displaystyle H}{\underset{\displaystyle H}{\mathrm{Si}}}\text{–O–M} + H_2 \quad (1)$$

In this report, we provide new evidence for the modification of oxide-free metal substrates with trihydridosilanes and propose a mechanism for the modification.

2. Experimental

2.1. Silane Synthesis

Hydridosilanes were synthesized by lithium aluminum hydride reduction of corresponding halosilanes or *alkoxysilanes* by the method previously reported [7].

2.1.1. 4-Bromobutylsilane

A 2-l, 3-neck flask equipped with a cooling bath, a magnetic stirrer, a pot thermometer, an addition funnel and a nitrogen protected dry-ice condenser was charged with 1000 ml of dry ether and 37.95 g (1 mol) of lithium aluminum hydride. This mixture was stirred at room temperature until the lithium aluminum hydride was well-dispersed. 270.4 g (1 mol) of 4-bromobutyltrichlorosilane were added over a period of 1 h into the above mixture while maintaining the pot temperature below 40°C. The pot temperature was maintained at 40°C for an additional 4 h after the addition of 4-bromobutyltrichlorosilane was complete. A clear top organic layer was separated from the bottom phase containing salts by cannulation. The organic layer was slowly added into 1000 ml of cold 2 N HCl at a pot temperature of 5°C. The mixture was then poured through glasswool into a separatory funnel, the aqueous layer was discarded and the organic layer was dried over sodium sulfate for 5 min.

The dried organic layer was distilled through a Vigreux column. 98.4 g (yield: 60%) of clear liquid were collected at 44–46°C at 20 mmHg: GC indicated 98.7% purity, density of the product at 25°C: 1.193 g/cm^3. IR and NMR results were consistent with the target structure.

2.1.2. 11-Bromoundecylsilane

A 1-l, 3-neck flask equipped with a cooling bath, a magnetic stirrer, a pot thermometer, an addition funnel and a nitrogen protected dry-ice condenser was charged with 250 ml of dry ether and 9.49 g (0.25 mol) of lithium aluminum hydride. This mixture was stirred at room temperature until the lithium aluminum hydride was well-dispersed. 92.16 g (0.25 mol) of 11-bromoundecyltrichlorosilane were added over a period of 30 min into the above mixture while maintaining the pot temperature below 40°C. The pot temperature was maintained at 40°C for an additional 2 h after addition of 11-bromoundecyltrichlorosilane was complete. A clear top organic layer was separated from the bottom phase containing salts by cannulation. The organic layer was slowly added into 300 ml of cold 2 N HCl at a pot temperature of 5°C. The mixture was then poured through glasswool into a separatory funnel, the aqueous layer was discarded and the organic layer was dried over sodium sulfate for 5 min. The dried organic layer was distilled through a Vigreux column. 32.6 g (49%) of slightly brown liquid was obtained at 101°C at 0.5 mmHg: GC indicated 98.1% purity, density of the product at 25°C: 1.020 g/cm^3. IR and NMR results were consistent with the target structure.

2.1.3. 1,4-Disilabutane

A 22-l, 4-neck flask equipped with a heating mantel, a mechanical stirrer, a pot thermometer, an addition funnel and an argon protected Vigreux column with distillation head was charged with 9000 ml of diethylene glycol dimethyl ether. 569.3 g (15.0 mol) of lithium aluminum hydride was portionwise added over about 4 h. The mixture was stirred at room temperature until the lithium aluminum hydride was well-dispersed. 2659.4 g (7.5 mol) of bis(triethoxysilyl)ethane were then added over a period of 4 h while maintaining pot temperature below 55°C. The pot temperature was maintained at 45°C for an additional 2 h after addition of bis(triethoxysilyl)ethane was complete. 565 g (83%) of clear liquid was collected over 6 h at 0–5°C with 50 mmHg. GC indicated 97.6% purity, density of the product at 25°C: 0.697 g/cm^3. IR and NMR results were consistent with the target structure. (Caution: Warm vapors, approximately 50°C, of 1,4-disilabutane in partially evacuated systems were observed to ignite when air was bled back to the system.)

2.1.4. 1,10-Disiladecane

A 12-l, 4-neck flask equipped with a heating mantel, a mechanical stirrer, a pot thermometer, an addition funnel and a nitrogen protected dry-ice condenser was charged with 4800 ml of tetrahydrofuran. 303.6 g (8.0 mol) of lithium aluminum hydride were added over about 3 h. The mixture was stirred at room temperature until the lithium aluminum hydride was well-dispersed. 1755 g (4.0 mol) of bis(triethoxysilyl)octane was added over a period of 3 h while maintaining pot tem-

perature below 55°C. The pot temperature was maintained at 45°C for an additional 3 h, and then 1400 ml of dry hexane were added to the above mixture. This mixture was then slowly added into 4000 ml of cold 2 N HCl at a pot temperature of 10°C. The aqueous layer was removed through separation funnel and the organic layer was dried over sodium sulfate for 10 min. The dried organic layer was distilled through a Vigreux column. 577 g (82%) of clear liquid were obtained at 35°C at 0.3 mmHg: GC indicated 98.0% purity, density of the product at 25°C: 0.772 g/cm^3. IR and NMR results were consistent with the target structure.

2.2. Substrates

For contact angle experiments, gold coated glass slides (W-GOG-75-1.1 from Gelest Inc.) — 50 nm gold on aluminosilicate glass and 2.5 nm titanium adhesion layer between glass and gold — were used as received. Titanium foil (0.5 mm thick, 99%) was purchased from Goodfellow. For XPS and all other experiments with gold and titanium substrates, metal films were prepared by physical vapor deposition (PVD) on silicon wafers. Silicon wafers were used as silicon substrates.

2.3. Substrate Preparation

Prior to deposition silicon and titanium substrates were pre-cleaned by immersion in 1% hydrofluoric acid (HF) for 2 min or 5 s, respectively or by exposure to hydrogen plasma where noted.

2.3.1. Surface Modification for Contact Angle Experiments

Surface treatment was performed as spin-on or immersion deposition utilizing 0.2 M silane solutions in heptane at room temperature or vapor phase of the neat silane at 80°C. After deposition they were subjected to the following protocol: heptane rinse, followed by 5 min sonication in heptane, followed by 5 min sonication in D.I. water.

2.3.2. Surface Modification by Vapor Phase

A stainless steel tube with an inner diameter of 7.1 cm and a length of 30.5 cm was used as a reactor. A stainless steel sample holder ($2'' \times 6''$, flat on top) was placed in good contact with the inside bottom of the tube reactor. Chamber base pressure was less than 0.001 torr. An isolation valve sits between chamber and vacuum pump to isolate the chamber when necessary for dosing experiments and system venting. The silane is contained in a glass bubbler. Valves and delivery lines were all stainless steel. Argon carrier gas (purity: 99.999%) flow rate was controlled by a mass-flow-controller.

All substrates were pre-cleaned with 1% HF. The chamber was filled with argon and held 24 h before removing the samples. In order to evaluate the effects of sample temperature and exposure time on the adsorption process, the following process parameters were evaluated: substrate temperature of 23–400°C, including experiments involving ramped substrate temperatures, employing ramp rates of 3–13°C/min. Exposure times of 30 min to 24 h were investigated.

2.4. Contact Angle Measurement

Water contact angles were measured with a Ramé-Hart Goniometer Model 100. All values reported are an average of all treatments.

2.5. XPS Investigation

XPS was performed using a Thermo VG Scientific Theta Probe X-ray photoelectron spectroscopy (XPS) system, with a spatial resolution < 50 μm and angle resolved XPS depth profiling capability using a 2-D multi-channel detector. A 300 W monochromatic Al K_α line was employed.

3. Results and Discussion

A variety of metal substrates were screened for interaction with octylsilane, octyldimethylsilane, octadecylsilane and octadecyldimethylsilane. The contact angle of water was measured on substrates treated with silanes (neat and in solution) at room temperature and elevated temperature. Variations of the contact angle after rinse steps and time were recorded.

The treatment of titanium metal with octadecylsilane and octadecyldimethylsilane in solution depicted in Fig. 1 is representative. Both the alkyldimethylhydridosilanes and the alkyltrihydridosilanes impart hydrophobicity to metal substrates, but trihydridosilanes are more effective than monohydridosilanes. The maximum contact angle for the trihydridosilanes requires an induction time, while no change with time is observed for the monohydridosilane. These results are similar for neat deposition on gold at 80°C depicted in Fig. 2, although the time to achieve maximum contact angle is shortened. An induction time is also observed at 80°C in the case of titanium (Fig. 3). Comparison of octadecylsilane deposition on titanium,

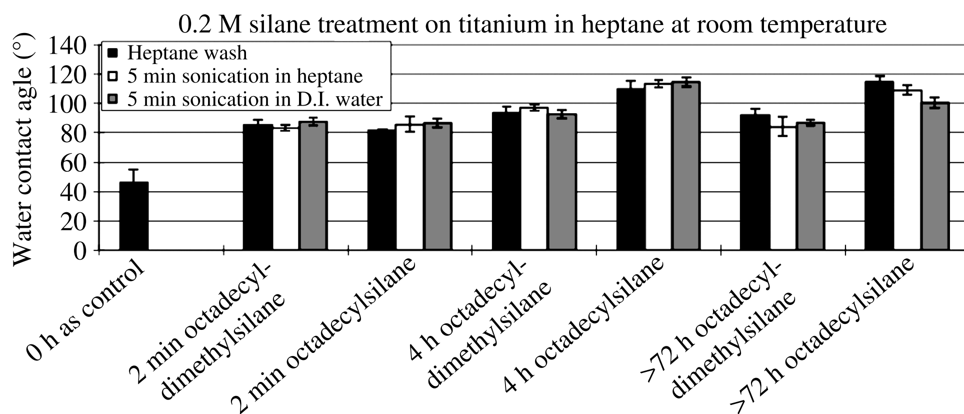

Figure 1. Contact angle of water on titanium metal after room temperature exposure to octadecyldimethylsilane and octadecylsilane solutions in heptane, for 2 min, 4 h and >72 h. After exposure substrates were (1) rinsed with heptane, (2) rinsed with heptane followed by sonication in heptane, (3) rinsed in heptane, followed by sonication in heptane, followed by sonication in deionized water.

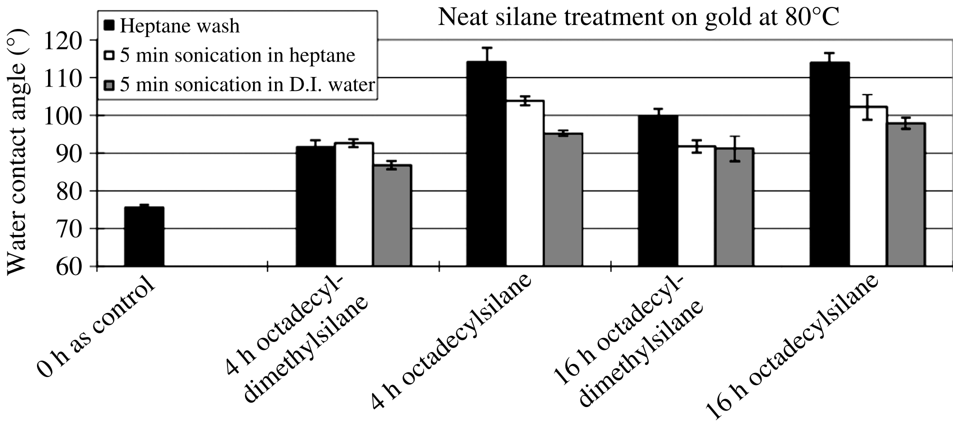

Figure 2. Contact angle of water on gold after 80°C exposure to neat octadecyldimethylsilane and octadecylsilane, for 4 and 16 h. After exposure substrates were (1) rinsed with heptane, (2) rinsed with heptane followed by sonication in heptane, (3) rinsed in heptane, followed by sonication in heptane, followed by sonication in deionized water.

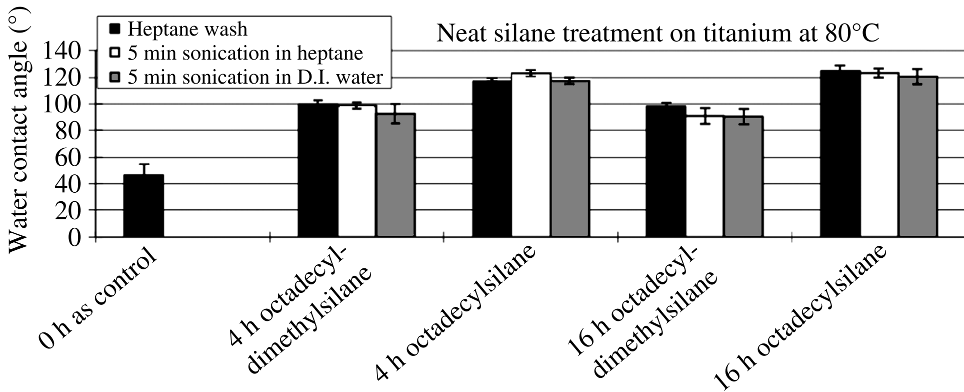

Figure 3. Contact angle of water on titanium metal after 80°C exposure to neat octadecyldimethylsilane and octadecylsilane, for 4 and 16 h. After exposure substrates were (1) rinsed with heptane, (2) rinsed with heptane followed by sonication in heptane, (3) rinsed in heptane, followed by sonication in heptane, followed by sonication in deionized water.

depicted in Fig. 1, with octylsilane on titanium, depicted in Fig. 4, demonstrates similar changes in contact angle with time. Figure 5 depicts octadecylsilane deposited on gold from solution at room temperature and demonstrates a contact angle profile comparable to neat deposition on gold.

While the differences in hydrophobicity may possibly be explained by differences in adsorption between the trihydridosilane and dimethylhydridosilane due to possible steric constraints imposed by methyl groups, it would seem unlikely since the methyl groups would also contribute to low surface energy. The induction period to achieve maximum contact angle by the trihydridosilanes may be accounted

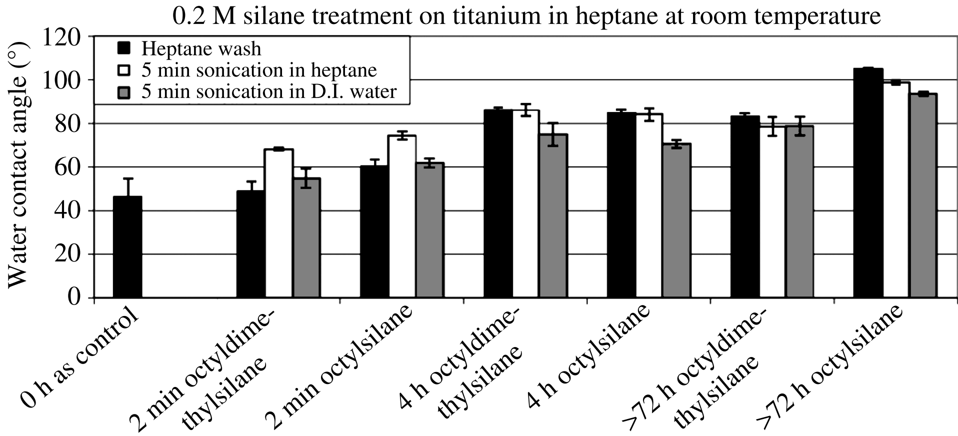

Figure 4. Contact angle of water on titanium metal after room temperature exposure to octyldimethylsilane and octylsilane solutions in heptane, for 2 min, 4 h and >72 h. After exposure substrates were (1) rinsed with heptane, (2) rinsed with heptane followed by sonication in heptane, (3) rinsed in heptane, followed by sonication in heptane, followed by sonication in deionized water.

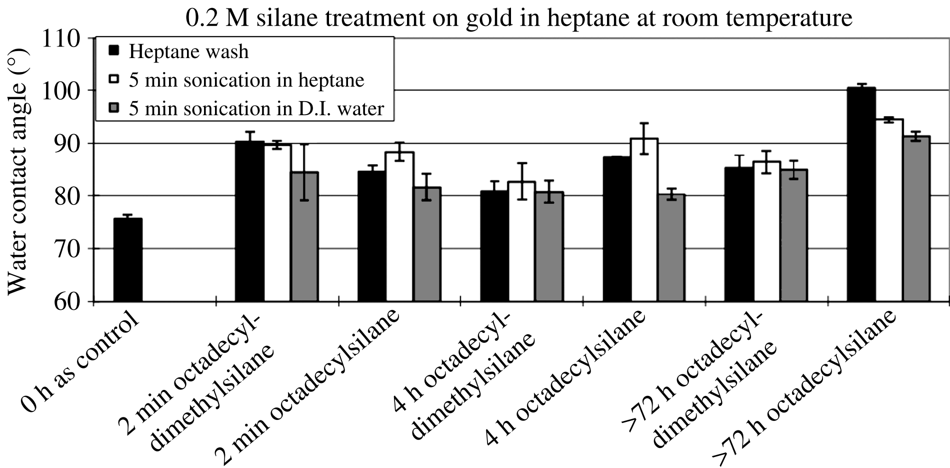

Figure 5. Contact angle of water on gold after room temperature exposure to octadecyldimethylsilane and octadecylsilane solutions in heptane, for 2 min, 4 h and >72 h. After exposure substrates were (1) rinsed with heptane, (2) rinsed with heptane followed by sonication in heptane, (3) rinsed in heptane, followed by sonication in heptane, followed by sonication in deionized water.

for by a time requirement for self-assembly but it is not clear why this would occur for the trihydridosilane and not the monohydridosilane. It is also possible that post-deposition oxidation processes related to the metal could affect surface energy as a function of time. However, there is consistency between readily oxidized titanium and relatively inert gold and oxidative processes, whereby, in general, surface energy increases with time. The induction period for maximum hydrophobicity is the same for both C_8 and C_{18} substituted trihydridosilanes which suggests that self-

assembly which is usually driven by alkyl chain length is not the primary reason for the time dependent changes in contact angle.

In studies of trihydridosilane interaction with gold, Owens *et al.* [8] noted the absence of hydrogen bound to silicon on silane treated gold substrates and likened it to the absence of hydrogen bound to sulfur for the alkylthiol treated gold substrates. The observation that a trihydridosilane (three hydrogens bound to silicon) would have similar behavior to an alkylthiol (one hydrogen bound to sulfur) initially appeared to be consistent with our observations. Upon further consideration, this appeared to be inconsistent with the observation that the monohydridosilanes, with one hydrogen bound to silicon and therefore more similar to the alkylthiols, did not perform as effectively for modifying substrates. Tunneling AFM (TAFM) of alkylsilanes on metal substrates would be anticipated to provide the most direct information, but as noted by Owens *et al.* [8], the observation of self-assembled monolayers (SAMs) on metal substrates by TAFM is difficult due to tunneling current requirements [9]. In studies concerning the synthesis of Pd nanoparticles in the presence of trihydridosilanes, Chauhan *et al.* similarly failed to observe silyl hydride absorption bands in infrared studies [10].

Two series of experiments were undertaken in an attempt to elucidate the mechanism for the modification of substrates by trihydridosilanes. In the first series, we synthesized 4-bromobutylsilane and 11-bromoundecylsilane in order to provide a tag for XPS detection. In the second series we synthesized α,ω-bis(trihydridosilyl)alkanes in order to amplify the silyl hydride density at the substrate.

XPS was used to analyze the Br 3d photoelectron peaks for 11-bromoundecylsilane-treated substrates. The Br fingerprint spectrum indicates that the bromoalkylsilane adsorbed onto all substrates evaluated. After liquid phase treatment, the pre-rinse initial peak intensities of all substrates were roughly equivalent. The greatest difference between pre-rinse and post-rinse Br 3d spectral intensity, employed as an indication of binding strength, was observed between clean silicon and silicon dioxide surfaces. These results are depicted in Figs 6 and 7 and indicate a moderate to strong interaction with silicon and only a slight interaction with silicon dioxide. The Br 3d pre-rinse and post-rinse spectra of 11-bromoundecylsilane on titanium are shown in Fig. 8 and are similar to that observed for gold. Among the metals tested, post-rinse intensity strength was in the order Ti $>$ Si $>$ Au. These results are interesting in that they correlate to the relative dissolution volumes of hydrogen in metals [11]. However, there appears to be more than one bonding environment for the bromine atom in the various substrates suggesting that in addition to the Br–C bond associated solely with the alkyl chain, there are other substrate-dependent interactions of the bromine atom.

The second series of experiments utilized 1,10-disiladecane and 1,4-disilabutane treatments on gold substrates. The resulting adsorbed species were profiled using angle-resolved XPS (ARXPS), where the effective information depth is adjusted by changing the relative take-off angle of the sample, thus changing the source of pho-

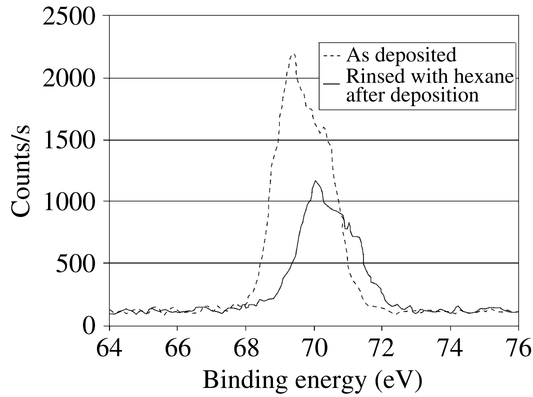

Figure 6. 11-bromoundecylsilane deposited on silicon (XPS-Br3d).

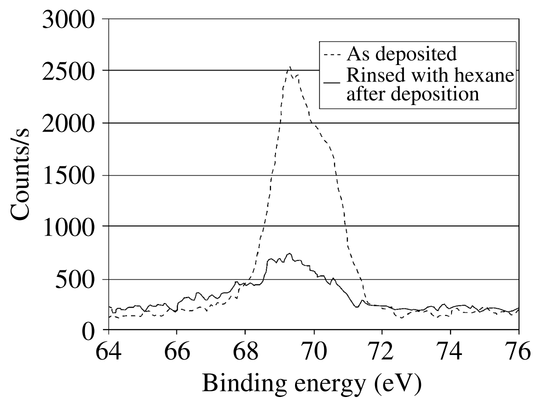

Figure 7. 11-bromoundecylsilane deposited on SiO_2 (XPS-Br3d).

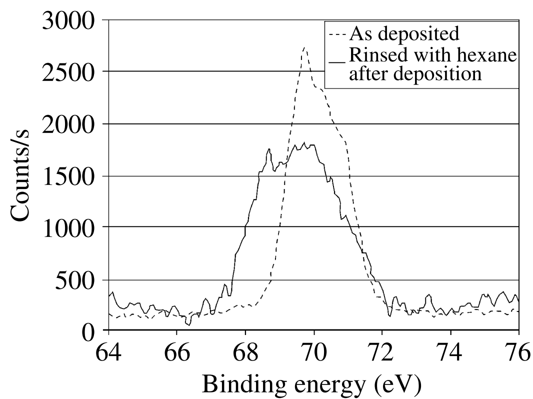

Figure 8. 11-bromoundecylsilane deposited on titanium (XPS-Br3d).

toelectron species with respect to depth. The results depicted in Figs 9 and 10 can be summarized as follows: The ratio of carbon to Si^{+4} is slightly higher than the stoichiometry required for disiladecane (4:1); Si^{+4} is observed in close proximity to the surface — at or above it; Si^0 is observed relatively deeper — at or below the surface. Au and O signals also originate from below the surface. Meanwhile, increased C noted above the surface is associated with the hydrocarbon bridge of the disiladecane molecule. Further, while perhaps within the limits of experimental error, the oxygen atom concentration most closely correlates with the silicon atom concentration but has a greater tendency to increase with depth. The presence of oxygen atoms indicates that there is a mechanism for oxidation that must be associated with the silane, since gold does not form oxides under the experimental conditions.

In the previous studies of alkylsilane deposition on gold, investigators were unable to detect hydrogen bonded to silicon by reflection absorption infrared spectroscopy (RA-IRS). In general our Fourier transform IR (FTIR) spectroscopy studies were able to detect deposited silanes, although barely above noise level, but were unable to detect hydrogen bonded to silicon. In the case of 1,4-disilabutane treated substrates, we were able to detect weak absorptions for hydrogen bonded to silicon, as shown in Fig. 11. These weak absorptions provide some insight into the fate of the silicon hydrides. The absorption of a hydrogen associated with $R\mathrm{SiH}_3$ is normally in the 2160 cm^{-1} region. While the spectrum shows a very weak absorption at 2160 cm^{-1}, it shows a stronger adsorption in the 2060 cm^{-1} region. This result is comparable to adsorption of methylsilane on silicon observed by Spencer and Nyberg [12] and Shinohara *et al.* [13] and attributed to formation of methylhydridosilylene on the surface. Shinohara *et al.* observed no evidence of silylene formation during deposition of trimethylsilane at room temperature. In a study of methylsilane and disilane adsorption and dissociation on Si(100), Xu *et al.* concluded that pentacoordinated silicon in $-\mathrm{SiH}_3$ groups was involved in non-dissociative chemisorption [14]. It can be tentatively concluded that the difference in surface modification between the alkyldimethylhydridosilanes and the alkyltrihydridosilanes is that a dissociative adsorption mechanism driven by the loss of hydrogen is available in the case of the alkyltrihydridosilane.

Recalling from the angle-resolved XPS study that the oxygen concentration correlates with the silicon atom concentration, it is reasonable to suggest that one pathway for oxygen incorporation is the reaction of the silylene with atmospheric oxygen to form alkylhydridosiloxane or alkylsilsesquioxane. While the dominant pathway for oxygen incorporation is from the alkylhydridosilylene, an additional pathway in which silicon atoms from the alkylsilane are injected beyond the topmost layer of gold with loss not only of hydrogen but also of organic substituents creates an alternate path for silylene formation and conversion to oxide. The loss of organic substitution on alkyltrihydridosilane being concomitant with silicon atom incorporation into the topmost layer of metals is consistent with a study of Menard *et al.* [15] in which methylsilane was reacted with a copper substrate at tempera-

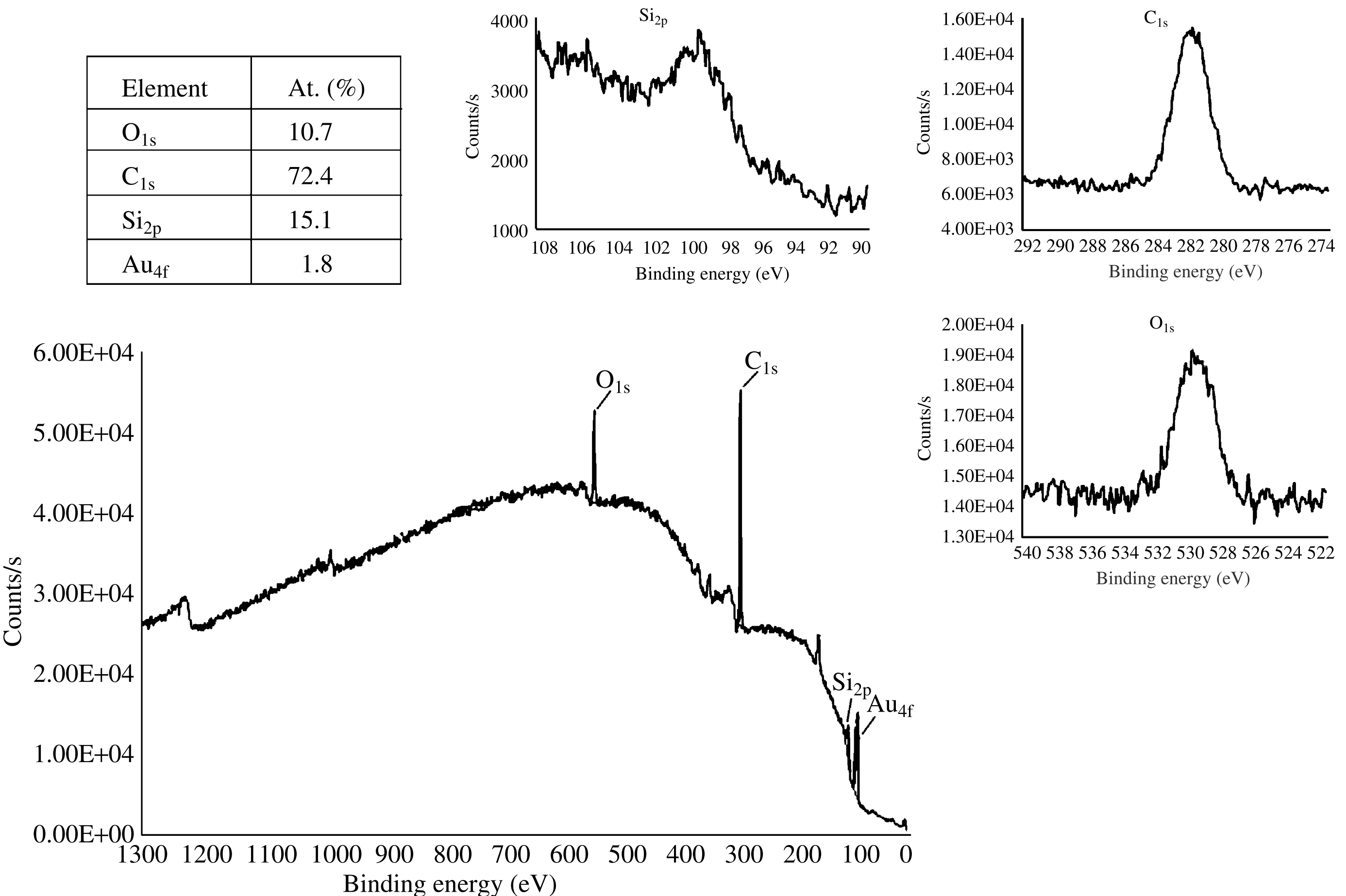

Element	At. (%)
O_{1s}	10.7
C_{1s}	72.4
Si_{2p}	15.1
Au_{4f}	1.8

Figure 9. XPS survey spectrum for 1,10-disiladecane on gold.

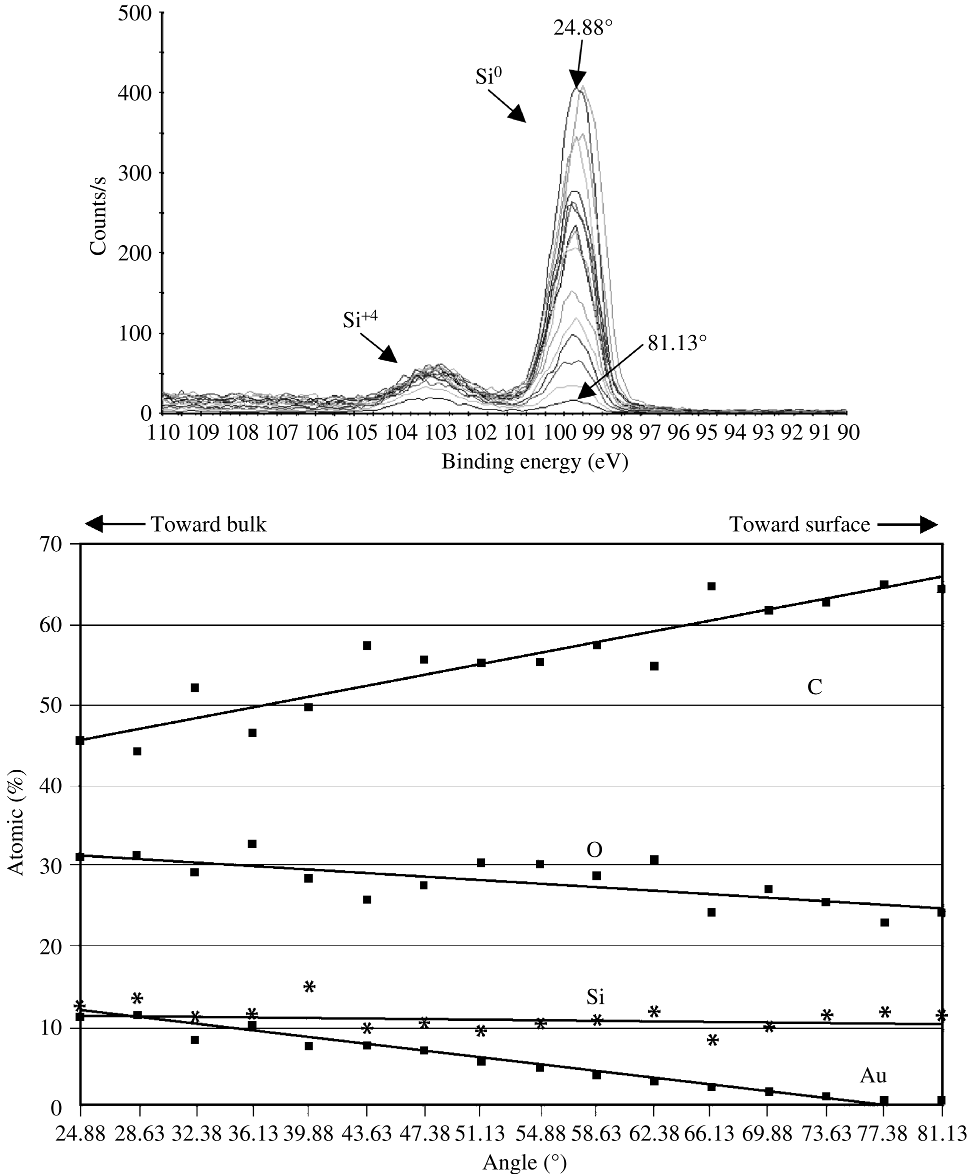

Figure 10. (top) 1,10-disiladecane on gold ARXPS Si_{2p} depth profile survey; (bottom) plot of overall compositional trends with respect to depth (take-off angle).

tures >200°C to form copper silicide. A study of the deposition of unsubstituted silane (SiH_4) on copper by electron energy loss spectroscopy (EELS) provides further supportive results as well as insight into the orientation of both the adsorbate and substrate [16], suggesting that the preferred orientation of the adsorbate is axial.

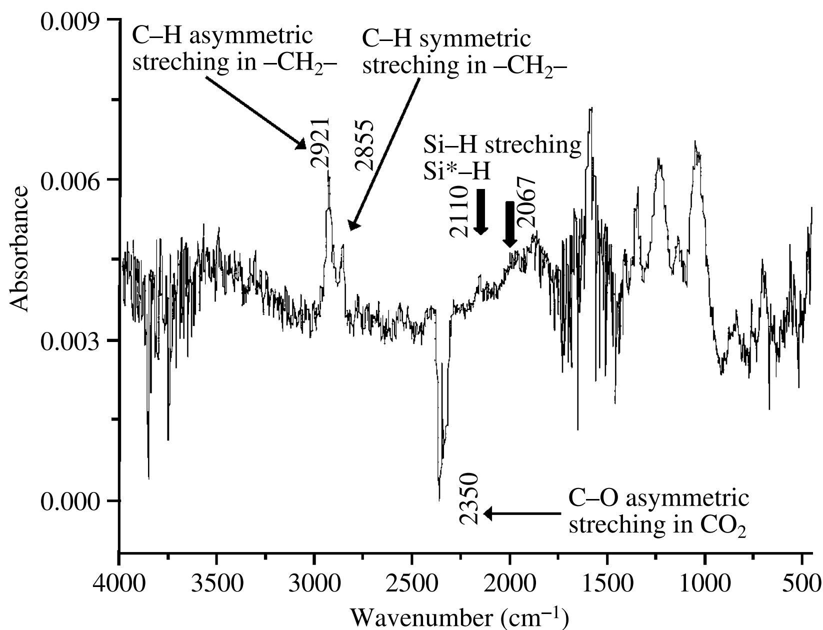

Figure 11. ATR-FTIR spectrum of 1,4-disilabutane deposition from hexane on titanium.

The oxidation of silylene in preference to hydrogen, generated from the hydridosilane, is consistent with studies of SiH_4 adsorption on palladium [17].

In the context of the literature cited, the data obtained in this study suggest the following mechanism:

(1) Trihydridosilanes adsorb in a perpendicular orientation to the surface with a hydrogen coordinated to a surface atom. Most likely the adsorption is at a site of a surface defect associated with a strained bond.

(2) The silane reorients, allowing coordination with a second surface atom.

(3) Dehydrogenation of the silane occurs with formation of a silylene in what can be regarded as a dissociative-adsorption process.

(4) Restructuring of the surface atoms is induced by the silylene, creating new strained bonds and vacancies allowing insertion of the silicon atom into the topmost layer of the metal.

(5) If sufficient strain is induced, the silicon atom may insert beyond the topmost layer into the substrate bulk, but the organic substituent is lost.

(6) Silylene reacts with oxygen on exposure to air, forming silsesquioxanes or, in the metallic bulk, oxides.

4. Conclusion

Alkylhydridosilanes interact with a variety of oxide-free metal surfaces. Alkyltrihydridosilanes react more strongly than alkyldimethylhydridosilanes. The adsorption of alkyltrihydridosilanes on metal appears more likely when a metal has the ability to adsorb or coordinate with hydrogen. It is proposed that the key step in chemisorption of trihydridosilanes involves dissociative-adsorption of the alkyltrihydridosilane with either the release of hydrogen or hydrogen absorption by the metal substrate. The results suggest a possible pathway for the precise formation of functional structures on metal substrates at the nanoscale using sequential and hierarchical fabrication methodologies.

References

1. K. L. Mittal (Ed.), *Silanes and Other Coupling Agents*. VSP, Utrecht (1992).
2. K. L. Mittal (Ed.), *Silanes and Other Coupling Agents*, Vol. 5. VSP/Brill, Leiden (2009).
3. R. G. Nuzzo and D. L. Allara, *J. Am. Chem. Soc.* **105**, 4481 (1983).
4. A. Ulman, *Chem. Rev.* **96**, 1533 (1996).
5. T. M. Owens, K. T. Nicholson, M. M. Banaszak Holl and S. Süzer, *J. Am. Chem. Soc.* **124**, 6800–6801 (2002).
6. A. Y. Fadeev and T. J. McCarthy, *J. Am. Chem. Soc.* **121**, 12184 (1999).
7. B. Arkles, J. Larson and Y. Pan, US Pat. 6,410,770 (2002).
8. T. Owens, S. Süzer and M. M. Banaszak Holl, *J. Phys. Chem. B* **107**, 3177–3182 (2003).
9. T. Owens, B. J. Ludwig, K. S. Schneier, D. R. Fosnact, B. G. Orr and M. M. Banaszak Holl, *Langmuir* **20**, 9636 (2004).
10. B. Chauhan, R. Thekkathu, L. Prasanth, M. Mandal and K. Lewis, *Appl. Orgaonomet. Chem.* **24**, 222 (2009).
11. M. Ya. Fioshin and M. G. Smirnova, *Electrochemical System in Synthesis of Chemical Products*. Publishing House “Chemistry”, Moscow (1985).
12. M. J. S. Spencer and G. L. Nyberg, *Surface Sci.* **573**, 151 (2004).
13. M. Shinohara, T. Maehama and M. Niwano, *Appl. Surface Sci.* **162-3**, 161 (2000).
14. J. Xu, W. J. Choyke and J. T. Yates Jr, *J. Phys. Chem. B* **101**, 6879 (1997).
15. H. Menard, A. Horn and S. Tear, *Surface Sci.* **585**, 47 (2005).
16. M. J. S. Spencer, G. L. Nyberg, A. W. Robinson and A. P. Stampfl, *Surface Sci.* **505**, 308 (2002).
17. D. Kershner and J. W. Medlin, *Surface Sci.* **602**, 786, (2008).